MICROCALORIMETER TECHNIQUES WITH THERMOELECTIC TRANSFER STANDARDS

Emil Vremera[1], Luciano Brunetti[2], Eugen Sfartz[3], Luca Oberto[2], Marco Sellone[2]

[1] *Technical University of Iasi, Faculty of Electrical Engineering*
Bld. Dimitrie Mangeron 53, 700050, Iasi, Romania
Tel: +40 232 278683; Fax: +40 232 237627; E-mail: evremera@ee.tuiasi.ro

[2] *Istituto Nazionale di Ricerca Metrologica (INRiM)*
Strada delle Cacce 91, 10135 Torino, Italia
Tel: + 39 11 3919333, Fax: +39 11 346384, E-mail: brunetti@inrim.it

[1] *Technical University of Iasi, Faculty of Mechanical Engineering*
Bld. Dimitrie Mangeron 61-63, 700050, Iasi, Romania
Tel/Fax:: +40 232 232337; E-mail: esfartz@mc.tuiasi.ro

Abstract **-** The paper describes the realization process of the high frequency power standard with a twin broadband microcalorimeter designed for effective efficiency measurement of power sensors based on thermocouples. The process includes the important step of the microcalorimeter self-calibration and auxiliary *S*-parameter measurements necessary for evaluating the system error correction. Besides the previously used microcalorimeter measurement techniques, this paper proposes a measurement method able to lead to the final result overpassing the corrections step or the use of the extrapolated values.

I. Introduction

Microcalorimeter is a measurement system conventionally considered a primary power standard and in practice used for effective efficiency measurements of power sensors like thermistor mounts, which become primary transfer standards in this way [1]. Recent technique improvements, both hardware and software, consider thermocouple power sensors as a powerful alternative to the classical bolometric ones. Main difference from bolometer case is the missing of the dc bias power. These lead to low temperature development but heaving higher relative variation. Feeding lines have an important contribution to this variation and must be determined in a microcalorimeter calibration step for operating the system correctly. Coaxial twin microcalorimeter calibration uses the dummy load concept and *S*-parameter measurements for the error correction related to feeding line losses [2]. The uncertainties of $\pm 2\%$ at 2σ previously obtained for effective efficiency η_e [3] have been recently reduced to less $\pm 0.5\%$ on a frequency band of 26 GHz. An important part of this uncertainty comes from VNA measurements because the implied quantities are small but with great weight in the errors propagation law [2].

II. Microcalorimeter and Thermocouple Power Sensors

The measurement system we are considering is schematized in Fig. 1 and is based on a dry adiabatic calorimeter. Its thermal load consists of a complex of two twin sensors, one of which is alternatively supplied with *HF* and *LF* or *DC* power through an insulating coaxial line. The other sensor is never energized during the calibration process and works only as thermal reference mass or dummy load. Anyway, this cold sensor may become the sensor under test (SUT) without open the microcalorimeter, it being usually a twin sensor. This possibility may be considered for saving time in the calibrations. The thermal insulation of the microcalorimeter load is obtained with a complex of aluminum-copper-aluminum shields separated by Polyurethane foam. The copper-shield is actively controlled in temperature by means of Peltier elements which provides a temperature stability of the inner shield at few mK.

The feeding lines are made of two sections of coaxial line fitted with connectors and exhibiting a high thermal insulation to the external environment. Conversely, in the section communicating with the external environment (*1-st Sect.*), only the inner conductor is a thermal insulator. This particular allows filtering better the thermal noise coming inside from the environment, because it is more easily conveyed on the thermal ground.

The microcalorimeter thermopile consists of independent two series of Copper-Constantan 98 thermojunctions. Combining the signal from the two-thermojuction series, we obtain the temperature difference between the SUT and the dummy sensor, which is proportional to the SUT effective efficiency.
The system is under computer control and all measurement steps are automatic, excluded the connection of the sensors to the test port.

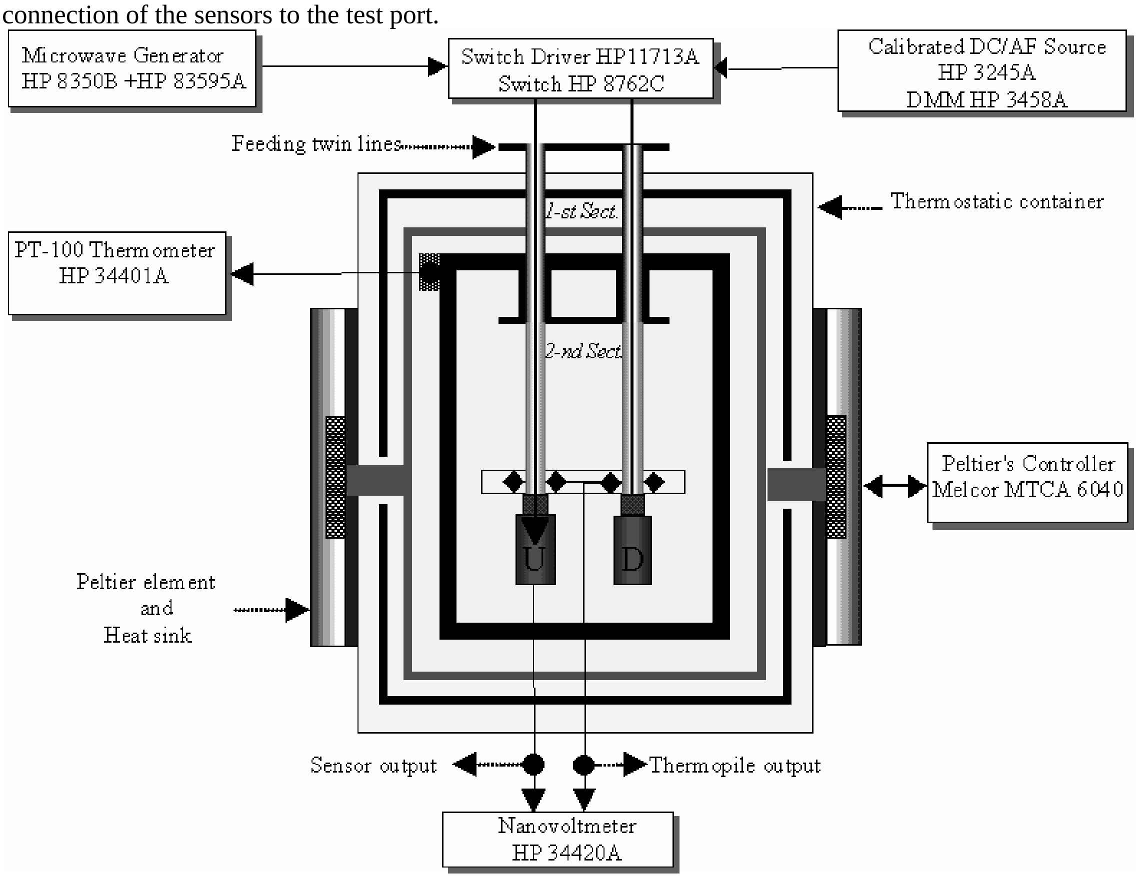

Fig. 1. Scheme of the INRiM coaxial line microcalorimeter.

A. Long-term Measurement and Calibration

After *HF* or *REF*-power is applied to the SUT through the feeding line, the thermopile output *e* begins to follow an increasing or decreasing exponential trend, tending toward finite asymptotes. Only the *e*-values corresponding to a thermal equilibrium and therefore near the asymptotes are meaningful for our purpose. As these values are obtained after several time constants τ of the system, they will be named long-time measurements. For understanding the heat distribution, it is convenient to split the voltage in two components [1], [4], one related to the power sensor and the other to the feeding line:

$$e = \alpha \Delta T = \alpha R\left(K_1 P_{inS} + K_2 P_{IL}\right) \tag{1}$$

where:
- α is the Seebek coefficient of thermopile junctions;
- R, a conversion constant depending on thermodynamic parameters of the thermal load;
- K_1, K_2, coefficients that describe the power separation between SUT and feeding line and
- P_{inS}, P_{IL}, the power dissipated in the sensor and in the insulating line respectively.

The response of the thermopile is e_1 when *HF*-power is supplied to the hot mount and e_2 when an equivalent *REF*-power is substituted. Long-time measurements of e_1 and e_2, at condition the SUT output V_0 = *const.*, may be conveniently combined in the following ratio e_R

$$e_R = \frac{e_2}{e_1} = \frac{P_{inS}\big|_{REF}}{P_{inS}\big|_{HF}} \frac{1 + K\left(P_{IL}/P_{inS}\right)\big|_{REF}}{1 + K\left(P_{IL}/P_{inS}\right)\big|_{HF}} \Bigg|_{V_0 = const.} = \frac{\eta_e}{g}, \quad K = \frac{K_2}{K_1}, \tag{2}$$

that includes the power sensor *effective efficiency* η_e and the *microcalorimeter calibration factor g* respectively defined as:

$$\eta_e = \left. \frac{P_{inS}\big|_{REF}}{P_{inS}\big|_{HF}} \right|_{V_0=const.} \quad (3) \qquad \text{and} \qquad g = \frac{1+Ka_{HF}}{1+Ka_{REF}}, \quad (4)$$

where the coefficients a_{HF} and a_{REF}, related to transmission parameters of the feeding lines, are determinate by vectorial S - parameter measurements:

$$a_{HF\,\mathrm{or}\,REF} = \left. \frac{P_{IL}}{P_{inS}} \right|_{HF\,\mathrm{or}\,REF} = \left. \frac{1-|S_{21}|^2}{|S_{21}|^2} \right|_{HF\,\mathrm{or}\,REF} . \quad (5)$$

The accuracy of the g factor contributes almost completely to the total accuracy of the system, especially at highest frequencies, where the insulating line losses are of the same order of the sensor losses. Beside transmission parameter S_{21} measurement, the microcalorimeter calibration step needs K ratio determination. Calculating K is a difficult task because it requires a change of the microcalorimeter normal configuration. Hot sensor and dummy sensor must be disconnected and substituted by two short circuits having the same thermal mass and this could change the thermal behavior of the system, leading to erroneous values of the separation constants K_1 and K_2. However, supposing the thermodynamic condition of the system is left unchanged by this operation, the estimation of K factor is:

$$K = \frac{e_{2sc}}{e_2 - e_{2sc}} \frac{P_{inS}\big|_{REF;V_0}}{P_{inIL}\big|_{REF;SC}} . \quad (6)$$

The index SC denotes the feeding line termination condition. If the isolating line has power losses at the reference frequency of the same order as the high-frequency power losses, the K ratio can be obtained more accurately at the reference frequency.

From (5) and (6), we compute the g factor and, finally, the *effective efficiency* of the power sensor results from the equation (2).

B. Accelerated Microcalorimeter Measurement and Calibration

After each power exchange (HF→AC/DC or vice-versa) the long-time measurement case implies a waiting time that should be more or less ten system time constants before sampling the microcalorimeter thermopile output [1]. With a time constant of 30 minutes, 8 test frequencies and requiring 10 independent results, the overall necessary time is over 800 hours. More than one month is needed even with a continuous automatic measurement process. By reducing the measurement time at 1 to 3 time constants, the overall measurement time decreases drastically, but this method implies mathematical corrections [4].

For relatively short switching time (T_{SW}), the thermopile output does not directly provide the values e_1 and e_2 requested by (1). These values may be obtained from the maximum and the minimum values e_M and e_m of the thermopile output signal. The ratio e_R of the thermopile output voltages, which is equivalent to the long-term measurement as defined in (2), is therefore given by:

$$e_R = \frac{e_m}{e_M} \frac{1-(e_M/e_m)\exp(-T_{SW}/\tau)}{1-(e_m/e_M)\exp(-T_{SW}/\tau)} = e_\tau H_\tau , \quad (7)$$

where:

$$H_\tau = \frac{1-(1/e_\tau)\exp(-T_{SW}/\tau)}{1-(e_\tau)\exp(-T_{SW}/\tau)} \quad (8)$$

is a correction factor depending both on the switching time and the microcalorimeter time constant.

The power separation coefficient K is possible to be found in the same manner as previously described. Using the same switching time like in the measurement case, this coefficient will result:

$$K = \frac{e_{M_{SC}}}{e_m - e_M \exp(-T_{SW}/\tau)} \frac{P_{inS}\big|_{REF}}{\left(1-|S_{12}|^2|S_{21}|^2\right)P_{inIL}\big|_{HF}} \ \text{(a) or } \ K = \frac{e_{msc}}{e_m - e_{msc}} \frac{P_{inS}\big|_{REF}}{P_{inIL}\big|_{REF}} . \ \text{(b)} \quad (9)$$

From (5) and (9.a) or (9.b), we compute the g factor. Finally, the *effective efficiency* of the power sensor will be computed, in this case, by the following equation:

$$\eta_{\mathrm{eff}} = e_R\, g = e_\tau H_\tau\, g . \quad (10)$$

Instead of using the correction factor H_τ, it is possible to compute the thermopile output voltage ratio from the extrapolated values which correspond to the long-term measurements case. This yields the use of a nonlinear fitting algorithm like Levenberg-Marquard or trust-region [5], [6], for a simplified model of the microcalorimeter. If a little bit more detailed model for the microcalorimeter is chosen, the fitting law becomes more complicated and new parameters will appear [6]. Fortunately, these parameters have a true physical signification and the computed corrected results become more accurate [5], [6], [7]. In Fig. 2, the extrapolated values of the experimental accelerated measurement data, computed from the fitting laws is represented together with the experimental data. A very good result of the fitting process is noticed; no visible differences are present. Since there are two main parts which contribute to the heat developing, the power sensor and the insulated line, we can model this by a sum of two exponentials containing two different time-constants [6]:

$$\text{fittedmodel}_2\,(x) = a_1 \cdot \exp(-b_1 \cdot x) + a_2 \cdot \exp(-b_2 \cdot x) + c \qquad (11)$$

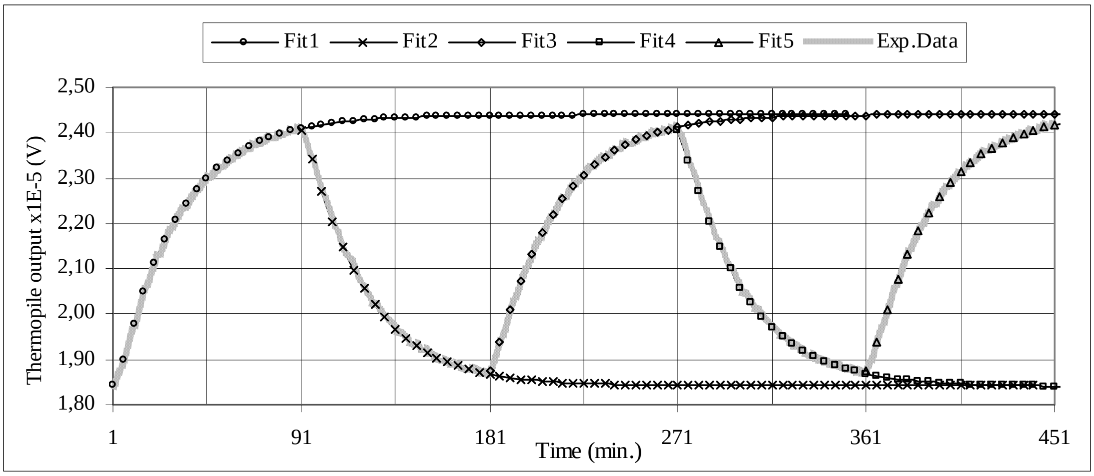

Fig. 2. Extrapolated thermopile output waveform resulted by nonlinear fitting law method applied in the accelerated-measurements case for time constants τ_1 = 29,06 minutes and τ_2 = 4,47 minutes, a switching time T_{SW} = 90 minutes and an extrapolation time interval of 305 minutes.

The same result can be obtained with trust-region algorithm if it is used with the same options as in Levenberg-Marquard case. But Gauss-Newton algorithm is not convergent for many data sets [6].

III. Simultaneous Measurement and Calibration

In an almost ideal case, the thermal contribution of the feeding paths can become a common-mode quantity and can be rejected [8]. In order to reach such a case, the feeding paths must have equal insertion losses, the energy travelling through them must be the same, the thermopile must be perfectly balanced and the power separation coefficients set must be matched as good as possible. In a real case, we are more on less far from these conditions, [7], but a particular self-calibration method can be applied, based on the measurement set-up schematized in Fig. 3.

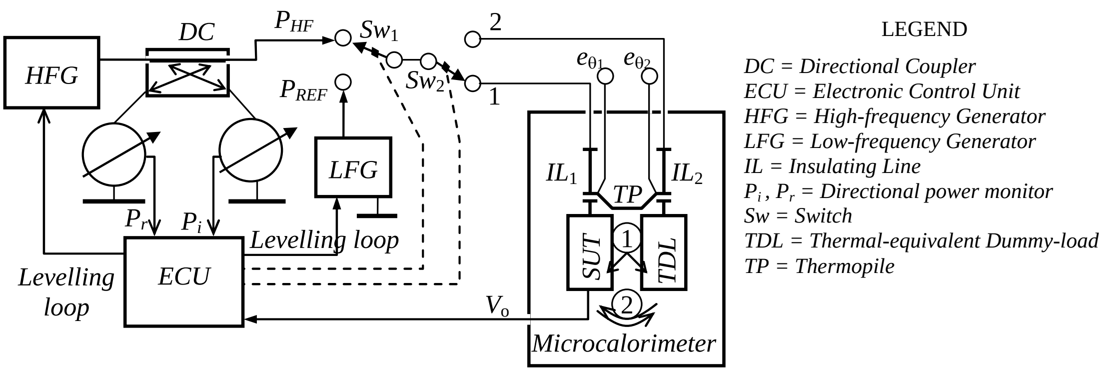

Fig. 3. Instrumentation set-up for simultaneous measurement and calibration method.

Two microwave coax switches, Sw_1, Sw_2, allow performing the measurement/calibration steps. The switching time of Sw_1 – between the reference power P_{REF} and the test power P_{HF} – is greater than the power sensor time constant. Conversely, the switching time of Sw_2 for power way selection – applied on *SUT* or *TDL* – is short with respect to the thermal time constant of the insulating lines IL_1, IL_2. The power level must be set two times greater than in the usual case. If an adequate power levelling algorithm, as that for keeping the same travelling energy on both paths, is applied, a part of the previous hypothesis is thus fulfilled. Measurement/calibration operations are repeated in two conditions:

- the 1st step, when IL_1 is terminated by *SUT* and IL_2 is short-circuited by *TDL*;
- the 2nd step, when IL_1 is short-circuited by *TDL* and IL_2 is terminated by *SUT*.

The thermopile *TP* works now as an asymmetric two channels device. Considering the asymmetries between the thermopile sections as well as in the power separation coefficients *K* and in the insulating line, (3) will become now a more general equation related to the effective efficiency η_e of the *SUT*:

$$1/\eta_e = \left.\frac{P_{inS}}{P_{REF}}\right|_{V_0=ct} = \frac{e_\theta(P_{HF})}{e_\theta(P_{REF})} - \frac{\alpha_1 R_1 K_{21}\left(P_{IL_{11}} - P_{IL_{12}}\right) + \alpha_2 R_2 K_{22}\left(P_{IL_{21}} - P_{IL_{22}}\right)}{e_\theta(P_{REF})}, \tag{12}$$

with $e_\theta(P_{REF}) = (\alpha_1 R_1 K_{11} + \alpha_2 R_2 K_{12})P_{REF}$ and P_{REF} an accurate **dc** or **lf** power level; the first index digit, 1 or 2, distinguishes the feeding paths and the second index digit refers to the measurement/calibration step. The last term in (12) is minimized by suitable microcalorimeter design and by an excellent power leveling loop. By controlling all implied quantities, this term becomes insignificant. Thus, the effective efficiency reduces to a simplified equation:

$$\eta_e = \left.\frac{P_{REF}}{P_{inS}}\right|_{V_0=ct} = \frac{e_\theta(P_{REF})}{e_\theta(P_{HF})}. \tag{13}$$

This expression of the effective efficiency is attractive because no correction terms are requested. In the uncertainty budget will appear only two terms, but every quantity in this ratio is obtained from two data sets corresponding to two measurement steps. Moreover, the neglected term can be estimated by its upper limit and will be assumed as type B uncertainty. A great attention must be paid to the thermopile, in order to be optimized from all points of view: signal/noise ratio, signal/offset ratio, absorbed energy and measuring sequences, resolution and accuracy, [7], [9].

IV. Conclusions

All the proposed methods may be efficiently used but the last one allows obtaining the microcalorimeter and transfer standard calibration data sets at one time. Because no corrections are necessary, the last method could be the real alternative to those based on corrections [4] – [7]. This solution is being verified at INRiM by using the same thermocouple power sensors whose effective efficiencies have been measured by means of another microcalorimeter in the classical way. Although the overall measuring requested time results almost the same like in the accelerated measurement case, the expected results and their uncertainties can be really improved. Moreover, the influence of the connector repeatability is partially taken in account.

References

[1] Fantom A., *Radiofrequency & microwave power measurement*, Peter Peregrinus Ltd., England, 1990.

[2] Brunetti L., Vremera E., A new microcalorimeter for measurements in 3.5-mm coaxial line, IEEE -Trans. Instrum. Meas., vol. 52, No. 2, pp. 320-323, April 2003.

[3] Janik D. et al., CCEM Key Comparison CCEM.RF-K10.CL (GT/RF 99-2) Power in 50 Ohm coaxial lines, frequency: 50 MHz to 26 GHz, Proc. of 27th CPEM, London, 2004.

[4] Vremera E., Brunetti L., Improvement of microcalorimeter measurements through data correction, Proc. of 16-th IMEKO TC4 Symposium, Athens, pp. 260-265, 2004.

[5] Brunetti L., Vremera E., New calibration method for microcalorimeters, IEEE Transaction on Instrumentation and Measurement, vol. 54, no. 2, pp. 684-687, April 2005.

[6] Vremera E. et al., Fitting curve method in accelerated microcalorimeter measurements, Bul. Inst. Pol. Iasi, vol. LII (LVII), fasc. 5, pp. 1115-1126, 2006.

[7] Brunetti L. et al., Microcalorimeter based on thermoelectric sensors, CPEM 06, Turin, pp. 658-659, 2006.

[8] Vremera E., Brunetti L., Another calibration method for microcalorimeters Proc. Of the 14-th IMEKO TC4 Symposium, Gdynia, Poland, pp. 71-74, 2005.

[9] Meijer G. C. M. and Herwaarden A. W. (Editors), Thermal Sensors, Institute of Physics Publishing, Bristol, 1994.